Orbital Debris Redirection and Thermal Reentry

D.O.T.T.S.

(Debris Orbital Tumbler and Thermal Sensor)

Our mission is to develop a concept toward a cost effective method for de-orbiting space debris that is too small to be tracked from Earth. Our secondary experiment's mission is to find more cost-effective materials for future experiments/projects in space that can sustain the effects of re-entry into Earth's atmosphere.

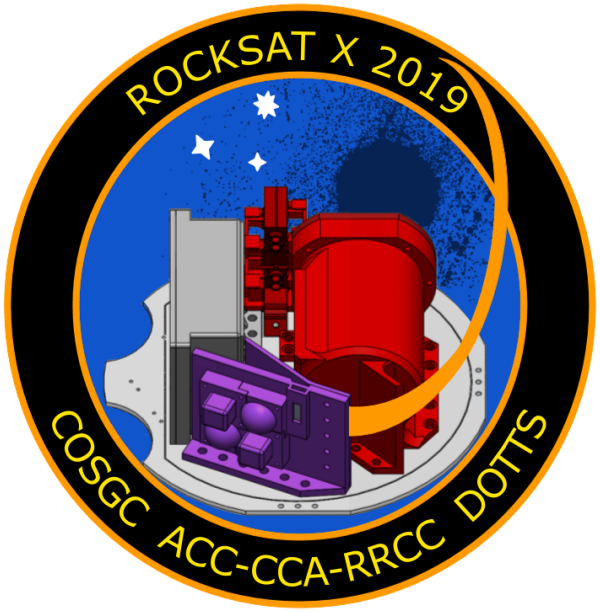

Stacie Barbarick[3], Bruce Bell[2], Cassidy Bliss[1], James Cook[3], Jack Dryden[1], Ethan Ford[1], Ruby Martinez Gomez[2], Joseph Harrell[2], Rhiannon Larsen[3], Ian McComas[3], Dallas McKeough[3], Henry Reyes[2], Nick Vail[1], Ryan Wade[2], Audrey Whitesell[1]

Victor Andersen[2], Jennifer Jones[1], Barbra Sobhani[3]

Arapahoe Community College[1], Community College of Aurora[2], and Red Rocks Community College[3]

09/30/2019

1.0 Mission Statement

We have designed a sounding rocket payload which contains two experiments. 1) Implementation and use of a static electric field to meaningfully impact the trajectory of a simulated space fragments. 2) Testing and documentation of key characteristic material properties on the effects of thermal reentry on multiple 3D printed structures of various filaments.

The 2017-18 Colorado Community Colleges RockSAT-X project demonstrated the influence of an electrostatic field on charged debris particles in microgravity. We will expand on this concept, with our primary experiment. The primary experiment will use an apparatus covered in rabbit fur attached to a mounted worm-drive motor to impart static charge on an adjacent polycarbonate plate. Using a linear sequence of specific timer events, four servos mounted within an ABS printed launcher will then propel a series of four small (6mm, 26 g) aluminum balls across the charged sheet at a muzzle velocity of less than one-inch per second. The first trial servo will launch the debris with no charge induced on the plate to serve as a control. A camera augmented with image processing code, mounted to the launcher and the payload deck will record changes to particle trajectory with video over-plotting onto a grid system. Limited data will be sent back via telemetry to confirm functionality and all image capture data will be stored on a secure digital (SD) card for analysis after payload retrieval. This will provide a proof of concept for a space cleanup method where the orbital velocity of space debris could be reduced, resulting in a decaying orbit where debris burns up in the atmosphere before reaching earth.

The use of additive manufacturing in aerospace applications is revolutionizing the industry and there is limited data on the thermal effects of reentry on additive manufactured materials, it is the focus of our secondary experiment [8]. Distinct filament structures, composed of either acrylonitrile butadiene styrene (ABS) or polyethylene terephthalate with a glycol modification (PETG) will be printed, measured and affixed to mounts installed on the payload deck. The vertical orientation of this deck allows for full exposure of all printed materials. Each design has a centered cavity containing resistance temperature detector (RTD) probes to measure internal temperature. The base of each shape has an interlocking design and screw holes to accommodate hardware attachment to the payload. Temperature data prior to launch will be collected as an internal baseline and temperature probes will continue to collect data through launch until splash down. Temperature data will be sent via telemetry to verify functionality and all temperature data will be stored on an SD card. Upon retrieval of the deck, printed structures will be analyzed qualitatively and compared to pre-launch, any deformation and change in shear strength will be analyzed and reported.

2.0 Mission Requirements and Description

According to the requirements established by the team, RockSAT, and Wallops, the following is a description of the general guidelines that were obeyed. Firstly, the mission parameters for the primary experiment were; can any significant change in the trajectory of non-ferrous materials passing through the field be observed using the tribo-electric effect. To do this, a charge generation needed to be established to create the static-electric field. A non-ferrous material would need to be used for the testing subject. The material would need to be a consistent and simple shape to evaluate. A launching mechanism would need to be designed to consistently launch the material at the same velocity and in the same trajectory. Wallops Flight Facility (WFF) also required that any deployable object have a max velocity of one-inch per second. A measurement system would need to be applied to track the progress of the material as it moves through the field. WFF requested that telemetry be used for the payload in the case that the rocket was not recoverable. As a convenience requirement, remove before flight software inhibitors were installed so that the material would not be ejected during testing procedures.

Secondly, the mission parameters for the secondary experiments were to receive qualitative and quantitative data on how well additive manufacturing materials (AMM) would survive reentry and how viable these materials would be as an inexpensive resource to use for payloads such as these. In order to accomplish this, the following parameters were set. Two different high temperature and widely available materials would be tested and chosen. The tests would consist of heating the materials in a forge, placing them in a vacuum, and simulate flash cooling by moving the forged materials quickly into an ice bath. Two simple shapes would be chosen for simple evaluation of the material. Accurate temperature data would need to be taken consistently throughout flight both inside the materials and outside as a control.

Thirdly, the payload has specified design and power requirements before being integrated into the rocket. The payload's center of mass would need to be within one-inch of the measured center of the plate deck. A height limit of 5 inches and weight limit of 15.0 +/- 0.5 lbs including the plate deck, and any other provided components such as the power and telemetry harnesses. In order to make sure there was no difficulty fitting into the skirt or messing with the stacking of the plates in the rocket a framed keep out zone on the edge of the plate was given as well. For power, the payload was given a limit of 28 Volts and 1 Amp Hour unless otherwise requested. The telemetry that was requested (Asynchronous, using RS232 protocols) was also limited to 19,200 bps baud rate. Any chemicals or biological materials would need to be approved by WFF before being allowed for flight.

Lastly, due to the nature of the experiment, an establishment of the effects of static electricity would need to be thoroughly explored and documented in order

to understand or expect any desired or undesired results of the experiment. To do this the general concept of attraction for non-ferrous materials to a static charge, as well as if this property is maintained in a vacuum environment.

3.0 Payload Design

The Community Colleges of Colorado payload designed to fly on the August 2019 RockSAT-X sounding rocket from Wallops Launch Facility, functions as a platform to begin the research in sub-orbital debris cleanup technologies which utilize electrostatic charges to interfere with small non-ferromagnetic materials in a vacuum, as well as the thermal capabilities of different 3D printed plastics during reentry into the atmosphere. These objectives are separated into two main experiments: primary and secondary experiment.

3.1 Full Assembly

The plate layout consists of five main regions, these are depicted in figures 5.1.1 through 5.1.4.

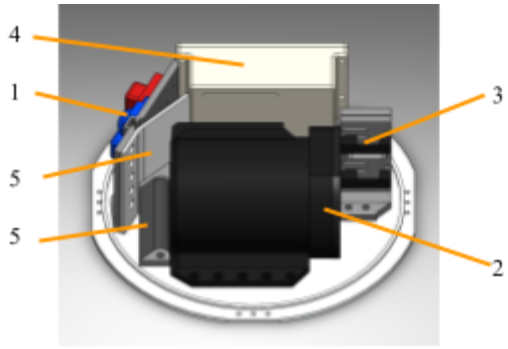

Figure 5.1.2 Front view of payload

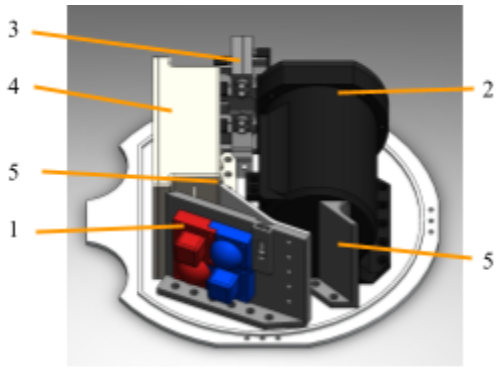

Figure 5.1.1 Right view of payload

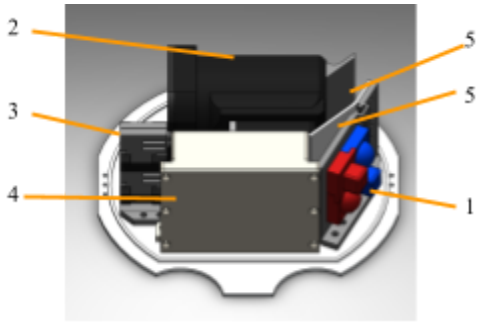

Figure 5.1.3 Back view of payload

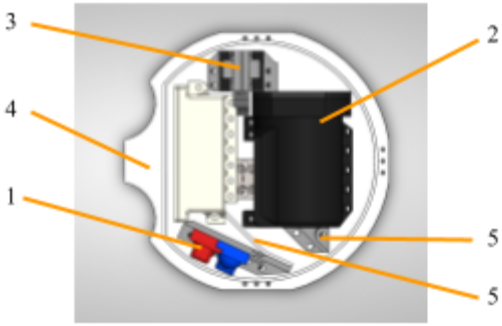

Figure 5.1.3 Top view of payload

Region 1 contains the secondary experiment; 3D printed structures, temperature probes, and surface mounts. Cubic and hemispherical structures will be printed in ABS and PETG to compare properties.

Region 2 is the earth atmospheric chamber (EAC) which houses the charging apparatus and polycarbonate charged plate. This chamber is to ensure static generation and is constructed primarily with 3D printed ABS. The lid is sealed with a rubber gasket and RTV silicone sealant.

Region 3 is the launcher tower made of ABS which houses the servos to launch the aluminum particles. This is also where one of two cameras will be mounted.

Region 4 is the location of the sealed electronics box, which will house the printed circuit boards (PCB), microprocessors, and SD cards. The box is constructed of 3D printed ABS. The lid is sealed with a gasket and RTV silicone sealant. The wires connected to the sides of the box and were sealed with RTV silicone sealant to waterproof.

Regions 5 are the deflector plates A and B, both made of ABS, to deflect particles launched and prevent them from continuing to register by the cameras.

3.2 Primary Experiment

The design for the primary experiment is broken down into three major components. The first being the electrostatic generator with a charge plate that produces an electrostatic field which is emitted from a flat plate (Figure 1).

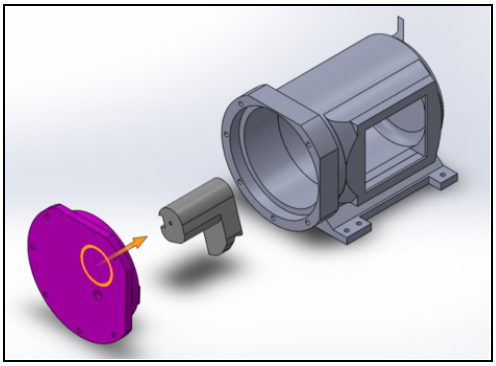

Figure 1: Exploded View of the EAC

The second component is the launcher which ejects the simulated debris samples at a rate of one-inch per second, with a straight trajectory parallel to the electrostatically charged flat plate (Figure 2). The launcher tower houses the test particles and the servos that will launch the debris. The servos will be held in place with a 3D printed plate that is screwed into the tower itself. Figure 3 shows an exploded front view of the launcher tower to highlight the plates.

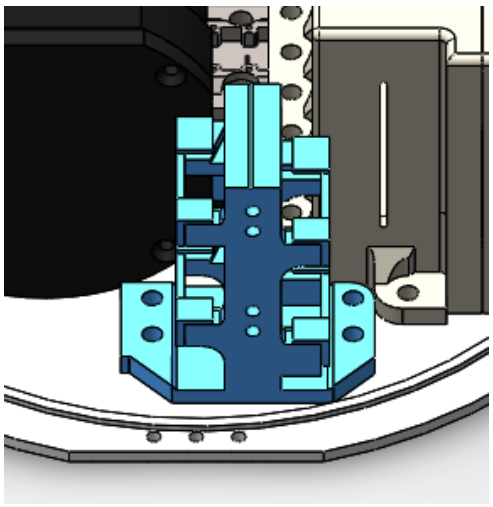

Figure 2: Assembled Launcher

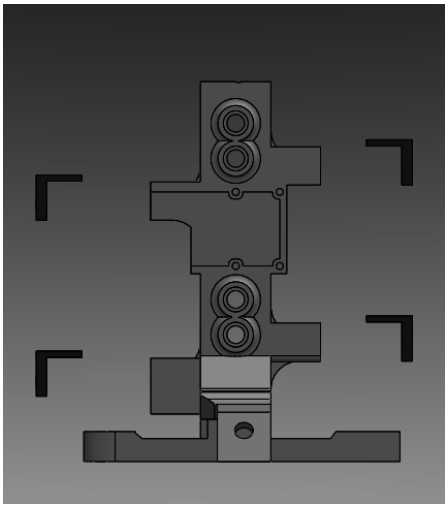

Figure 3: Exploded Front View of Launcher

The third component to support the primary experiment is the data collection method. The experiment's focus is to observe the trajectory of the debris samples as they enter the electrostatic field, this data must be stored and transmitted for post-flight analysis. This data collection is conducted through the utilization of two cameras whose field of view run perpendicular to each other, covering the are that the samples will travel (Figure 4).

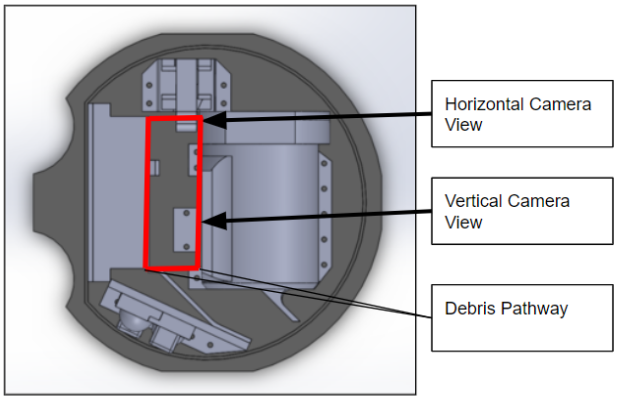

Figure 4: Top View of Payload

The primary experiment is designed to run three test trials, in addition to a fourth control trial. In figure 5, these four launches are illustrated in conjunction with the other operations in sequence. To ensure the best execution of the control data, it will be conducted first prior to any static charge generation on our payload.

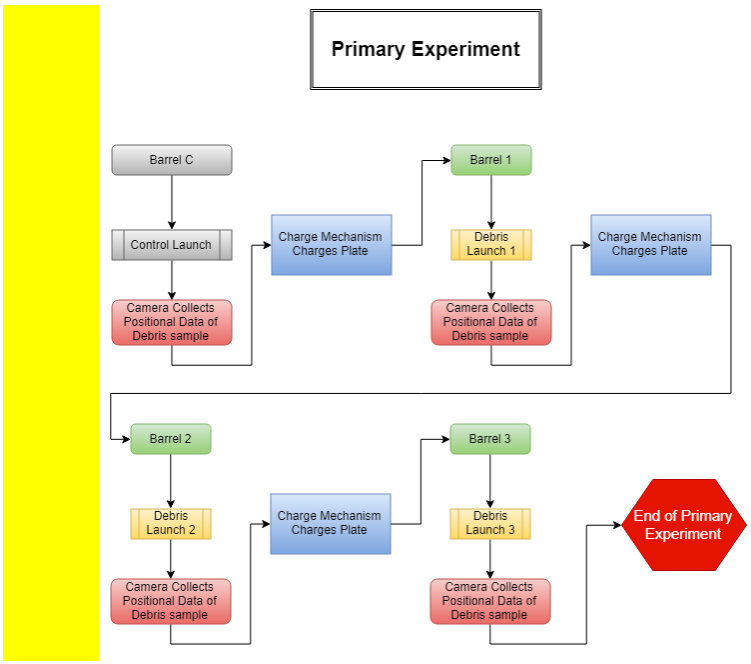

Figure 5: Primary Experiment System Block Diagram

3.3 Secondary Experiment

The secondary experiment is composed of three main components (Figure 6). 1) The deflector plate. 2) The secondary mount wall. 3) The 4 test subjects.

The deflector plate mounts to the secondary mount wall and ensures that the BBs ejected from the primary experiment is cleared from the cameras view point.

The secondary wall mount is mounted directly to the payload deck and holds the control probe as well as the 4 test subjects. The control probe is exposed to the external environments to compare external temperatures to the internal temperatures inside the shapes.

The final component of the secondary experiment is the test subjects. There are two shapes and two filaments. One cubical shape and one half sphere shape. There are two of each shape, one printed in PETG and one in ABS. The shapes have a wall thickness of 5 millimeters, and each contain a temperature probe on the inside to measure how heat resistive the printed material and shape is. In order to prevent the shapes from melting off of the payload, the base of each shape was

covered with an external fiberglass sheet (Figure 7). This ensured that the measured internal temperatures would be just from the exposed subjects and that upon splash down we could measure qualitative data.

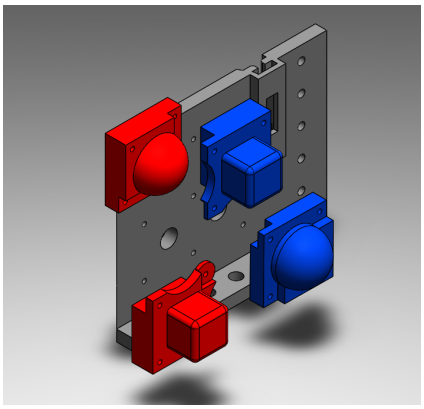

Figure 6.1: Exploded ISO View of Secondary

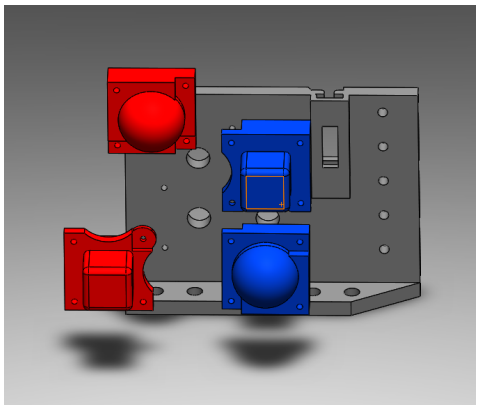

Figure 6.2: Exploded Angle View of Secondary

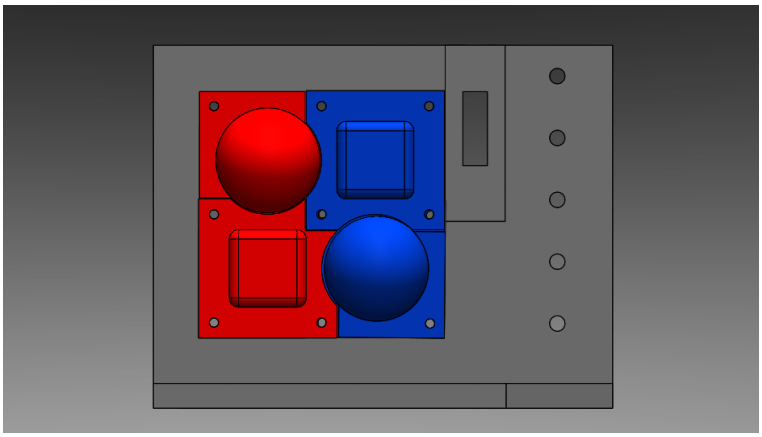

Figure 6.3: Assembled Front View of Secondary

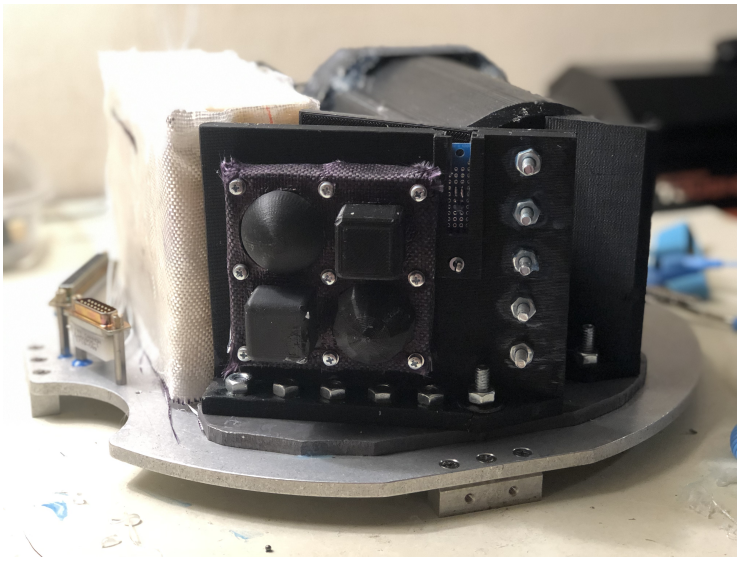

Figure 7: Assembled Flight Version of Secondary

4.0 Student Involvement

Sub-Team: Management

Ruby Martinez, Project Manager

Ruby is studying Aerospace Engineering at the University of Colorado - Boulder. Ruby served as lead for management and made sure that the progress of the payload was continued as well as ensuring all documentation was completed.

Stacie Barberick, Assistant Project Manager

Stacie is studying Materials Engineering at Minnesota State University - Mankato in a new cooperative and integrated program through Iron Range Engineering. She was involved in multiple aspects of the project. This ranged from management, to developing new concepts to the project, and being highly involved with design and mechanical components.

Sub-Team: Mechanical Design and Manufacturing

Bruce Bell, CCA - Mechanical Design Engineer

Bruce is studying at Metropolitan State University of Denver to obtain a Bachelor's degree in Mechanical Engineering and will then pursue a graduate degree at the University of Colorado Boulder. Bruce heavily supported the mechanical design team for both the primary and secondary experiment. Bruce was responsible for assembly, manufacturing testing, and 3D CAD.

Cassidy Bliss, ACC - Mechanical Design Engineer

Cass is studying at Red Rocks Community College transferring to CU Boulder to pursue a degree in Engineering Physics. She was a vital engineer within the primary experiment mechanical design team, as she was responsible for designing and testing multiple solutions for the payload. Cass also assisted in other sub-team objectives to help push this rapidly developing project along.

Dallas McKeough, RRCC - Mechanical Design Engineer

Dallas is studying to transfer from RRCC to Metropolitan State University to study Mechanical Engineering and hoping to pursue a graduate degree in space resources at Colorado School of Mines. During the project, Dallas was responsible for the organization and cohesiveness of the overall design for the payload, as well as the 3D CAD used for presentation, analysis, and construction of the payload.

Henry Reyes, CCA - Mechanical Design Engineer

Henry is studying at Community College of Aurora to transfer to University of Colorado at Boulder to study engineering physics. He assumed the secondary experiment and oversaw testing operations at CCA.

Nick Vail, ACC - Mechanical Design Engineer

Nick is studying at Red Rocks Community College to transfer to University of Colorado at Boulder studying astrophysics. Nick supported both primary and secondary designs and ensured the scientific quality was optimal.

Sub-Team: Electrical Design

Rhiannon Larson, RRCC - Electrical Design Engineer

Rhiannon will complete her Associates of Science with transfer designation in Physics from RRCC in Fall 2019 and transfer to Colorado School of Mines in Spring 2020. She worked on soldering and harnesses.

Ryan Wade, CCA - Electrical Design Engineer Lead

Ryan is studying at CCA to transfer to University of Colorado at Boulder to study electrical engineering. Ryan was heavily responsible for the design and manufacturing of the specialized PCBs accompanied with the multitude of other electrical components.

Audrey Whitesell, ACC - Electrical Design Engineer

Audrey is studying Physics at ACC and is planning to transfer to the Colorado School of Mines to study Mechanical Engineering. She was part of our electrical team and contributed to the testing and integration of the project. She also helped with the mechanical team.

Sub-Team: Software Design

James Cook, RRCC - Software Design Engineer

James is studying Aerospace Engineering and will be transferring to the University of Colorado - Boulder in the Spring. He was on the software team and was part of writing the code for data transfer and communication between the Raspberry Pis and Arduino micro controllers.

Joseph Harrel, CCA - Software Design Engineer

Joseph is studying Aerospace Engineering at the University of Colorado - Boulder. Joseph was essential in software production for the secondary experiment and conducted multiple tests.

Ethan Ford, ACC - Software Design Engineer

Ethan is studying Computer Science and is still unsure of where he will be transferring. He contributed to the software team and became a resource for things that need to be completed.

Ian McComas, RRCC - Software Design Lead

Ian is studying Aerospace Engineering and Applied Mathematics at the University of Colorado - Boulder. Ian lead code production and testing throughout the project.

5.0 Testing Results

5.1.1 Mechanical Design: Primary Experiment

Once the debris launcher was chosen as the testing methodology for static repulsion, several mechanical design factors had to be accounted for. The NASA Wallops Flight Facility requires any projectile shot from the sounding rocket to be at a velocity of less than one-inch/sec. To achieve this goal, the team was required to design and implement a mechanical gate, testing apparatus, and procedure.

After several iterations of design, a simple spoke mechanism was found to be the most effective and energetically inexpensive way to hold the debris in place until testing and to launch the debris with a controlled speed (Figure 8).

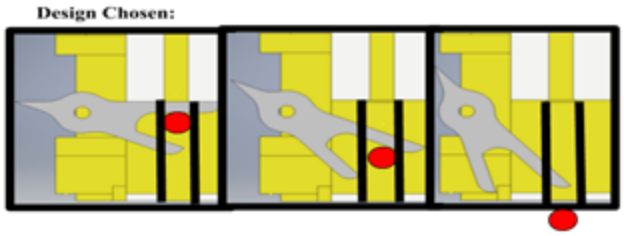

Figure 8: Mechanical launcher spoke design

The spoke was mounted to a servo which was programmed with a simple Arduino delayed step servo code. Measurements were initially taken with slow motion video and a meter stick along a track. Delays in the return of the servo arm were increased systematically the data collected is graphed below. A strong correlation between increased servo step delay and decreased velocity of the debris was observed (Figure 9).

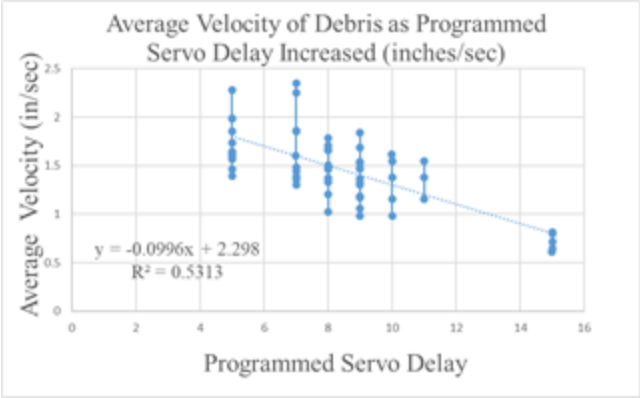

Figure 9: Testing Velocity of Debris

To increase trial speed and accuracy, a photogate was constructed with SparkFun photo resistors and a 3D printed launch tube with apertures for LEDs and sensors. To calibrate the ideal setting for photogate sensitivity, 30 trials at each of the sensitivity settings were conducted and graphed (Figure 10). We assumed the setting with the smallest average deviation within a data set was the most accurate and selected 910 as the setting to move forward with .

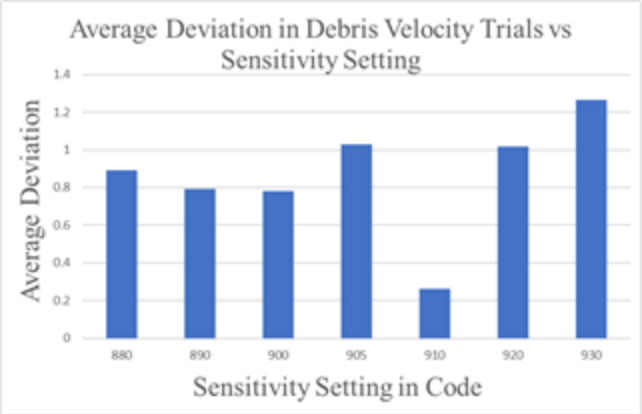

Figure 10: Testing Servo Sensitivity

To reduce variables in the calibration, we removed the servo and positioned the tube at a 20° incline. We then took 30 data points per sensitivity setting and graphed average deviation within each data set, in addition to the percent error found from calculating the ideal velocity we could expect with our parameters (Figure 11).

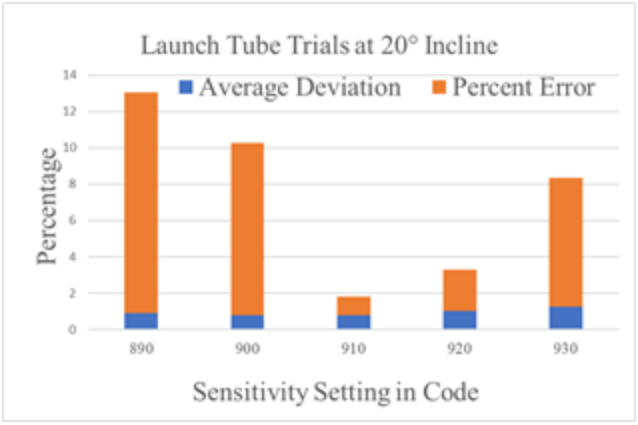

Figure 11: Decreasing Percent Error of Debris Speed

Again, we found the coded sensitivity setting at 910 to produce the lowest average deviation in addition to the lowest percent error. This allows us to use the settings of our test apparatus with confidence.

We determined the speed of the delay of the servo using our first plotted graph. Since we are required to have any deployments be one-inch per second or less, we used the delay setting of 15 milli-Seconds which gave us 100% of values well below the prescribed limit (Figure 12).

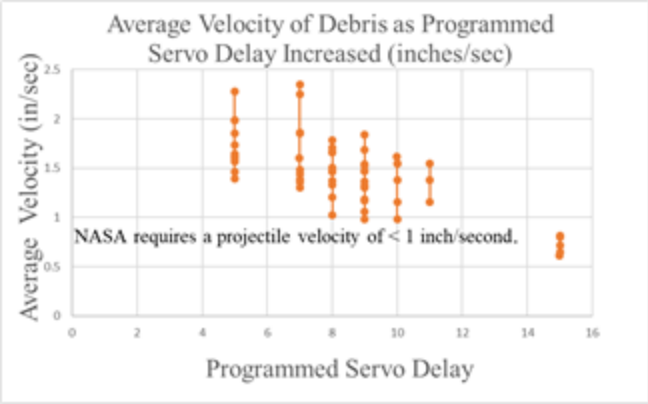

Figure 12: Average Deviation within trial sets vs sensitivity settings

As a result of testing regarding the charge imparted on the polycarbonate plate, we acquired instrumentation that measures electrostatic charge and will immediately begin testing charge generation, duration of charge, and radius of maximum influence on our debris particles.

Shake testing showed no visible fractures or defects; however, charging apparatus appeared to move during vibration and was moved further away from plate inorder to prevent premature static charging during launch.

5.1.2 Mechanical Design: Secondary Experiment

The limited data on thermal effects of reentry on affordable 3D printed materials allowed for more design freedom in the secondary experiment. Our goal is to test and record the effects of thermal build up on the rocket and its payloads during reentry in order to determine the viability of common 3D printed materials in future space flights. To this end, we compiled a list of potential filaments types and began elimination based on inherent material properties, limitations to equipment, and testing results.

We printed a variety of prototypes with varied parameters, such as wall thickness, material usage, and theoretical deterioration of melted filament and subjected them to high heat in a lab-built forge (Figure 13).

Figure 13: Lab Created Forge for Thermal Testing

Filament selections were based on access and availability with the intent to reduce research and development costs. Our initial tests included ABS and HIPS printed structures, exposed to heat in the forge for two minutes.

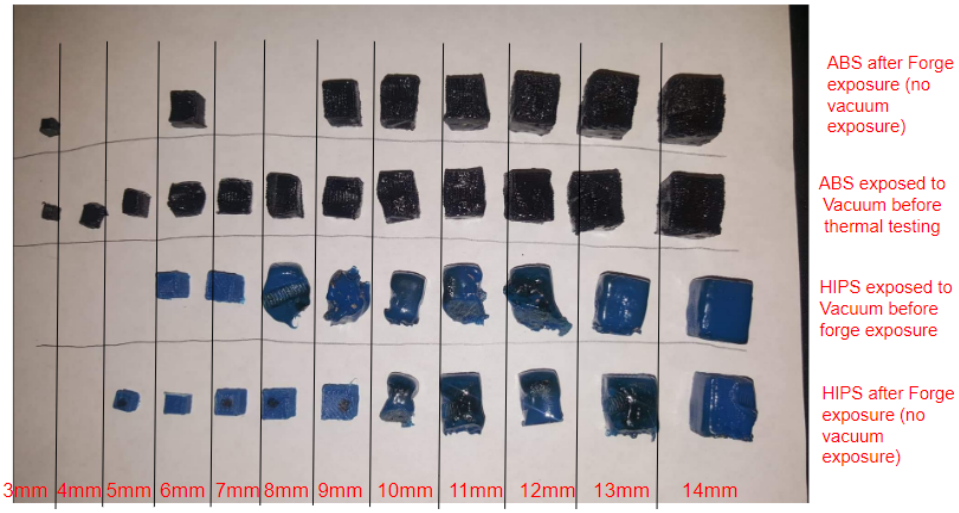

Figure 14: Qualitative data for ABS and HIPS materials exposed for two minutes.

The results of this testing seen in Figure 14, are as follows:

HIPS

Qualitative Results: The 13mm cube withheld its shape the best but high temperatures clearly penetrated through the cube. A different high temperature filament will be used for flight.

Quantitative Results: The 14mm cube lost the least amount of mass (0.027g) compared to the average (0.054g).

ABS

Qualitative Results: The ABS material held its shape both inside and out, suggesting less internal penetration.

Quantitative Results: Compared to HIPS, the ABS material lost less mass when exposed to the forge. The 14mm cube lost 0.004g compared to the average (0.0105g).

Variations that performed the best were then tested both in and out of a vacuum chamber. This was done to ensure the filaments used were porous enough to avoid explosion under extreme variations in atmospheric pressure. Inorder to replicate flight, the filaments were then exposed to the forge. Results are shown in Table 1 and Table 2.

AFTER-VACUUM												
Trial 1 (BLUE) HIPS												
Wall Thickness (mm)	Weight Before(g) (+- 0.001g)	Weight After(g) (+- 0.001g)	Temp. When Weighed (Degrees F)	Change in Weight	Time	Stone Stand Temp. Degrees (F)	Stone Stand Temp. Degrees (C)	Inside Temp. (F)	Inside Temp. End of Trail (F)	Object Temp. (40 sec before take out) (F)	Object Temp. End (10 sec before take out) (F)	Qualitative / Comments
9	1.426	1.41	74.1	0.016	1 min 10 sec	874	467.777 7778	624	590	788.5	798.3	Very gooey. If squeezed easily deformation...
10	1.825	1.787	75.2	0.038	1 min 10 sec	890.8	477.111 1111	628		819.1	826.3	Seems like the heat made it through
11	-			-	1 min 10 sec		0					
12	2.331	2.221	74.8	0.11	1 min 10 sec	943.9	506.611 1111	620	645	999	HI	Very Gooey while Taking out despite maintaining structure
13	2.874	2.845	74.8	0.029	1 min 10 sec	996.1	535.611 1111	618	610	820.9	887.4	
14	3.556	3.529	75	0.027	1 min 10 sec	979.5	526.388 8889	608	600	929.1	919	

Table 1: Trial data for HIPS after exposure to a vacuum chamber

AFTER-VACUUM													
Trial 1 (GRAY) ABS													
Wall Thickness (mm)	Weight Before(g) (+- 0.001g)	Weight After(g) (+- 0.001g)	Temp. When Weighed (Degrees F)	Change in Weight	Time	Stone Stand Temperature Degrees (F)	Stone Stand Temperature Degrees (C)	Inside Temp. (F)	Inside Temp. End of Trail (F)	Object Temp. (40 sec before take out) (F)	Object Temp. End (10 sec before take out)(F)		Comments
9	1.079	1.071	77.7	0.008	1 min 10 sec	817.3	436.3	611		758.5	732.9		Losing stiffness, easier to...
10	1.46	1.45	77.2	0.01	1 min 10 sec	835.3	446.3	617	590	763.5	789.8		Still has some stiffness not deformed at all...
11	1.847	1.84	77.7	0.007	1 min 10 sec	817.9	436.6	603	605	760.6	758.5		A little bit gooey but still maintained structure
12	2.381	2.378	77.9	0.003	1 min 10 sec	828.7	442.6	609	598	821.8	772.3		No real damage
13	3.007	2.976	77.9	0.031	1 min 10 sec	844.9	451.6	612	600	852.1	847.8		A little bit gooey however no real damage
14	3.641	3.637	78.6	0.004	1 min 10 sec	852.4	455.8	621	600	750	695		

Table 2: Trial data for ABS after exposure to a vacuum chamber

One concern we had was mounting 3D printed structures to the payload. The high (above 600°F) temperatures anticipated upon reentry, could cause 3D printed structures to dislodge. Since fiberglass is highly heat-resistant, we decided to use it to create a base cover that will allow exposure of the structure but with added protection to the base. This protective layer will help eliminate inaccurate data and ensure the experiment survives reentry.

The fiberglass cover was constructed out of molded, 5in x 5 in lightweight fiberglass solid mat. We tested the fiberglass cover by inserting it into the forge, forming a barrier between the torch and the RTD-100 temperature probes. The temperature probes printed numerical temperature data to the computer and the induced heat was read with a temperature gun. A temperature reading was taken every 30 seconds up to 3 minutes, to approximate anticipated reentry time. The results of this testing is summarized in figure 15.

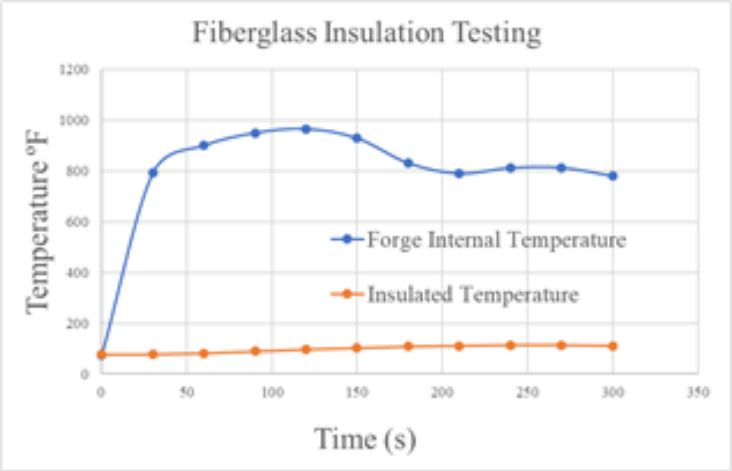

Figure 15: Testing fiberglass Insulative Properties

5.2 Electrical Design

The electrical design team was tasked with meeting the power needs of each experiment as it developed, while maintaining a strict power budget for the team to adhere to. We made decisions to accommodate the payload's restricted size and extreme environmental conditions, while adapting to design changes as the project progressed. We wanted to optimize payload deck space and make connection points accessible and reliable. We eliminated the use of multiple bulky buck converters and sizeable components with unnecessary utilities, by minimizing step down points and incorporating I2C components directly into our PCB design. Solid-state relays replaced mechanical relays for actuator activation, ensuring voltage reduction and reliability. All harness points and pin connection points were equipped with crimp pin sockets as opposed to solder joints, making boards and harnesses easier to access and change out during troubleshooting. A solid-state relay system was designed to switch the secondary experiment's power from the Wallop's timer event line to a self-contained LiPo battery, powering the thermal sensors for secondary experiment during descent. Detailed schematics were created using customized CAD libraries and 2D trace components which were edited to include specific order number details written into their code descriptions. An ever-evolving functional block diagram was referenced to assist the rest of the team as the payload was readied for subsystem integration (Figure 16).

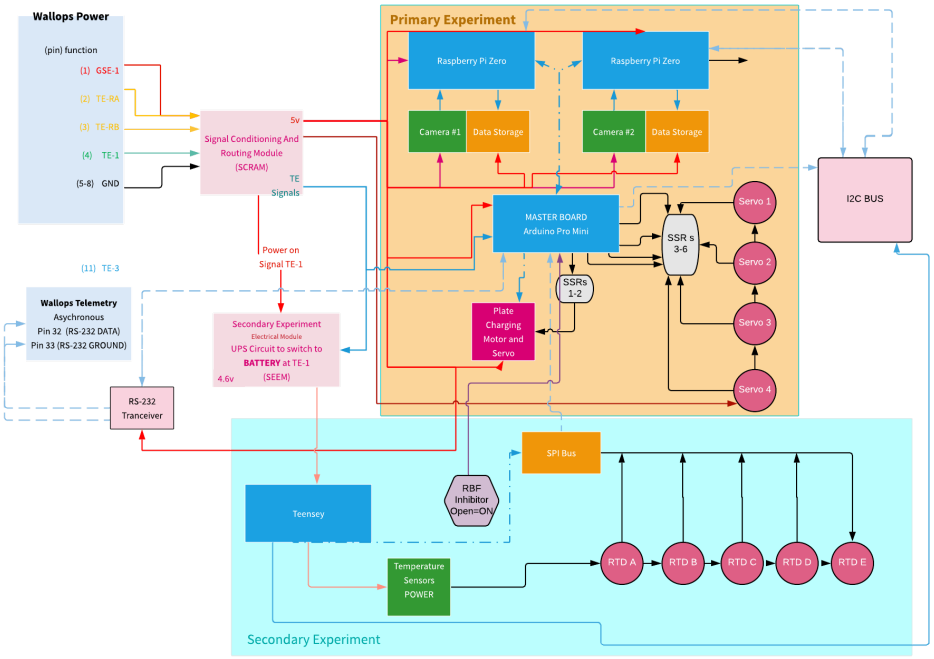

Figure 16: Electrical Functional Block Diagram

5.2.1 Electrical Design: Primary Experiment

The main electrical considerations for the primary experiment were pin availability and power budget. This experiment requires five servos and a motor which runs in sequence. Since each component requires several pins for power, data, and grounds, we decided to design and print customized printed circuit boards (Figure 17).

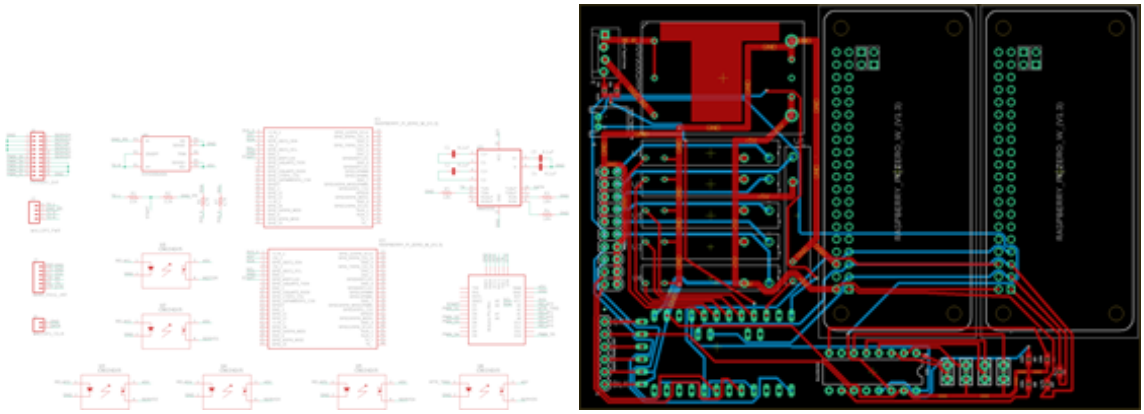

Figure 17: Autodesk Eagle Schematics for Primary Experiment PCBs

5.2.2 Electrical Design: Secondary Experiment

In order to record secondary data upon reentry, the electrical team designed an internal power supply and switch over circuitry because rocket power shuts off before reentry. The secondary experiment requires the use of five thermal probes and thus also requires increased access to power and input pins. Therefore, PCBs were also designed and implemented (Figure 18).

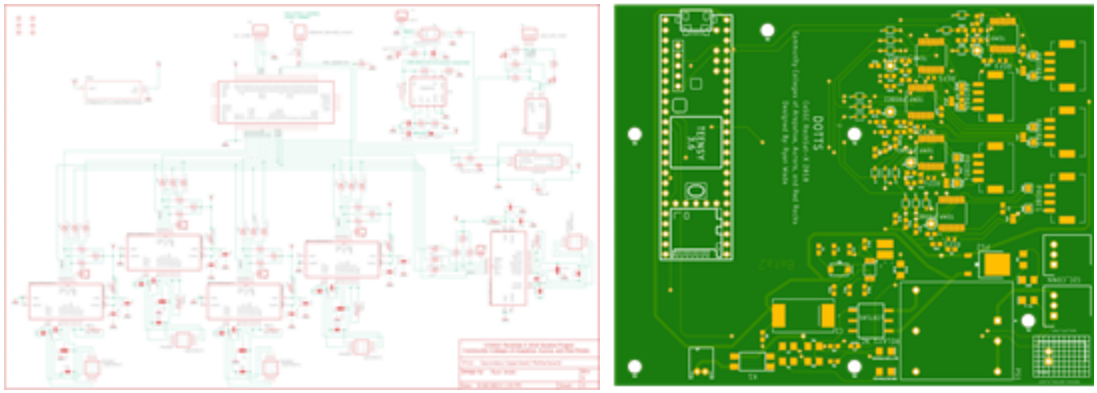

Figure 18. Autodesk Eagle Schematics for Secondary Experiment PCBs

All electronic components were closely inspected and individually tested to ensure there was no bridging or thermal damage from soldering. To further ensure protection from arcing or contamination, all electronic boards were conformally coated. In addition, all wiring insulation were tested to ensure safety and reliability of signal transfers.

5.3 Software Design

Software design required creative coding solutions to meet our unique data capture and storage needs, especially for our photo-recognition telemetry. We chose to code in Python because it has superior data processing, is open-source, and has access to high-level code libraries. Raspberry Pi Zero microprocessors and camera modules were chosen because of size and weight, but also processing capabilities. The Arduino platform is an ideal choice for designating events, so it was chosen as the master microprocessor and the Raspberry Pi's were designated slave microprocessors (Figure 19). Since there is no Linux driver that allows for this setup, the software team developed a work-around that allows the Pi's to function in this manner.

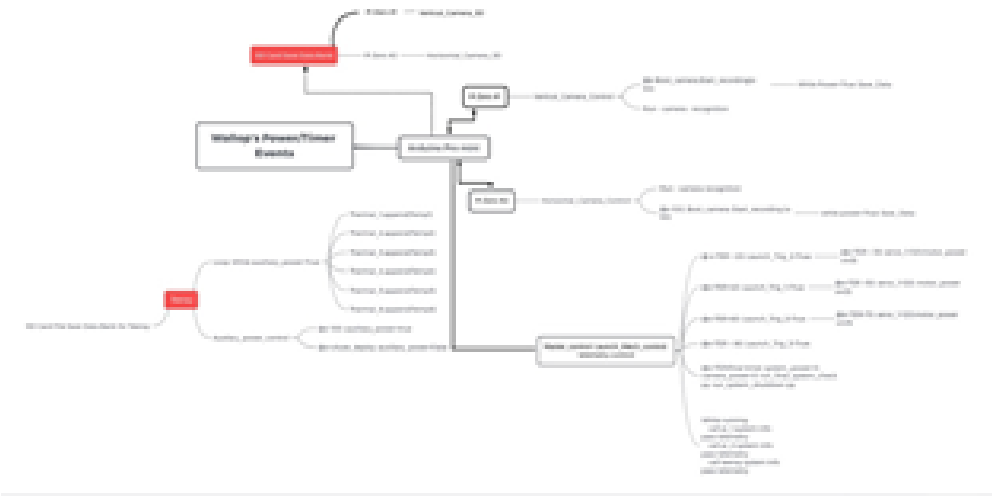

Figure 19: Software Functional Block Diagram

5.3.1 Software Design: Primary Experiment

The primary experiment required extensive programming for photo recognition software that will allow us to use a simplified matrix to track debris vector changes via telemetry (Figure 20).

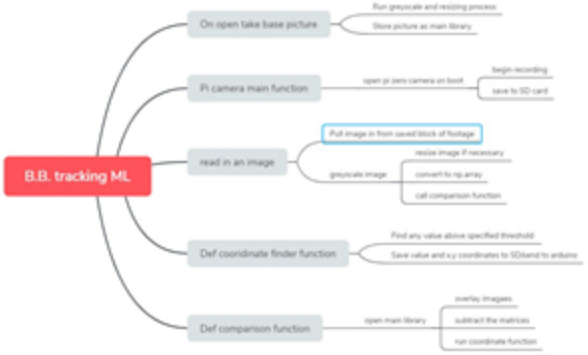

Figure 20: Photo Recognition Functional Block Diagram

An RGB sensor is a three-dimensional numerical space that combines red, green, and blue weights into numerical values that make up pixels. We can convert these values to grayscale by multiplying by a scalar and taking an average value to create a new two-dimensional image. Now the image is scaled from a 500 x 500 matrix via max pooling to a 100 x 100 matrix to lower processing time. A background image of a precisely created grid system will be stored as a library and all other images will overlay this background and comparisons made to x, y and pixel values. These comparisons allow us to determine distance in terms of pixels and create a 3D mapping of how the debris is moving through the field. The reduced data size allows for telemetry to be sent in addition to the video and

array set data stored on a SD card. Figure 21 demonstrates the photo recognition process.

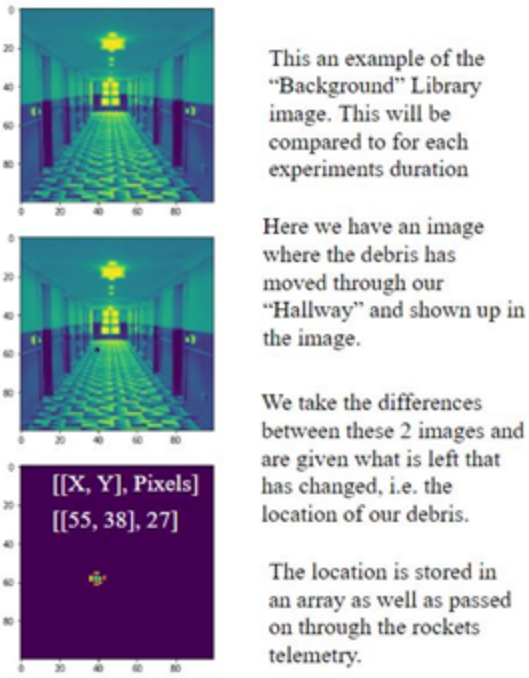

Figure 21: Photo Recognition Process

The two Raspberry Pi Zeros and an Arduino Pro Mini will be powered off the rocket's power, with a kill command assigned to preserve SD card data during splash down.

Major components:

- Raspberry Pi Zero #1 controls camera 1 to monitor debris vertically and saves data to SD card 1.
- Raspberry Pi Zero #2 controls camera 2 to monitor debris horizontally and saves data to SD card 2.
- Arduino Pro Mini controls all the servos and the motors and communication between our data processors and rocket telemetry.

Data will then be saved to its own SD card. It will also control timer events for the main systems.

6.0 Mission Results

Primary Experiment Analysis

Both the EAC and Electronics Chamber exterior of the primary experiment exterior survived reentry well, with minimum damage from reentry and

splashdown. There was evidence, however, that both of the chambers leaked water in upon the ocean splash or shortly thereafter.

The Launching System was severely damaged. The launching tower had broken in half. Three out of the four servos that were attached to the launching tower were lost, as well as the camera attached to the front of the launcher. We hypothesise that most of the damage was done to the launching system because of the heat from reentry and the impact upon splashdown, not prior to descend. The BB's were not inside what was remaining of the launch system and there was physical evidence from the servo that had remained that it had in fact turned as instructed in order to launch the BB. This was determined because of the angle of the lever mounted on the top of the servo.

The interior of the EAC had a substantial amount of water inside when taken apart. The charging plate itself had evidence of heat damage, and what appeared to be dust and small particles melted into the surface. This may have been indicative that the plate had attracted dust and small particles during the charging sequence of the primary experiment.

Aside from the qualitative data collected upon inspection of the payload after retrieval, we had two primary sources of data to analyze. The first was the telemetry data collected, which gave matrix values indicating position of the objects within the launching hallway after each launch. Within the telemetry data was also pixel values indicating the distance of the object being observed in relation to the camera. A "control" image was taken shortly before the launching of each test subject, this acted as a zero or a reference frame so when the BB is within the view of the camera it could accurately determine the position in the x-, y-, and z-direction

The second form of data collected was video footage taken during each launching sequence. Unfortunately, none of our footage of the launches showed evidence of the simulated debris moving in the view of the camera. There was also evidence of a crack on the camera that was attached to the launch tower (Figure 22). In test footage prior to the launch we found evidence that the crack had started before the launch and existed at least during our check-in at Wallops Island.

Our telemetry data showed matrix and pixel values indicating that objects were moving across the camera at the time the footage took place (during the launches). However, this was not consistent with the footage taken of the launches as there is no evidence of movement in the camera frame during this time.

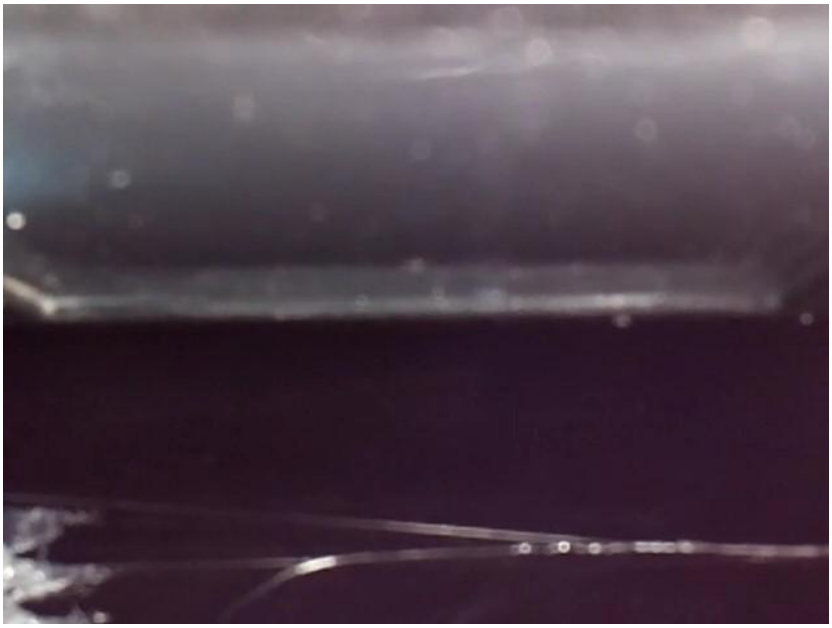

Figure 22: Visual Crack in Camera Lense

Secondary Experiment Analysis

Upon retrieval of the payload, one of the first things that was observed was the state that the 3D printed shape components were in. The structure of the 3D parts showed extremely promising results as from the outside view the shapes were not warped and barely had any considerable damage on them. From this first glance the hypothesis, that alternative low cost materials can be used in space and can resist the intense heat of reentry, was indicating promising results.

As seen in graph 1 there is a total of five lines, each corresponding to the indicated probes. The horizontal axis represents time in seconds ranging all the way from -300 seconds (GSE Start Up) through 0 seconds (time of launch) to after splash down and ending at approximately 2500 seconds. There is a clear distinction between the temperature collected from the control probe and the rest of the test probes. The maximum recorded temperature gathered by our control probe was 230°C, the minimum 0℃.

With regards to the PETG filament, the maximum temperature recorded was 49°C for both the cube and the spherical shapes, the minimum being 20°C and 19°C, respectively (Graph 3). This temperature data along with our qualitative analysis of the 3D parts was a very clear indication that the PETG filament is a very viable option as a low cost material for low earth orbit space flight. It also has the ability to shield about 181°C of heat, with only 5 millimeters of shell thickness.

For the ABS filament, the maximum temperature recorded was 48°C for the sphere and 38°C for the cube, while the minimum temperatures were 19 °C and 20°C, respectively (Graph 4). The ABS filament maintained its shape and

integrity, it also shielded about 182°C of heat, with only 5 millimeters of shell thickness.

As noted, the ability for both ABS and PETG to withstand reentry in both heat insulation and structural integrity cannot be denied. However, another question that needed to be answered is: Which material and shape resisted better?

Graph 2 shows a pretty big distinction in temperature detected. When analyzing the cubic structure, ABS shows that it did a better job at shielding the internal probe from heat compared to the PETG. The maximum temperature experienced by PETG was 11°C greater than the temperature experienced by ABS. Unlike the cubic structure, the sphere structures did not show any significant differences in temperature; both filaments experienced around 49°C.

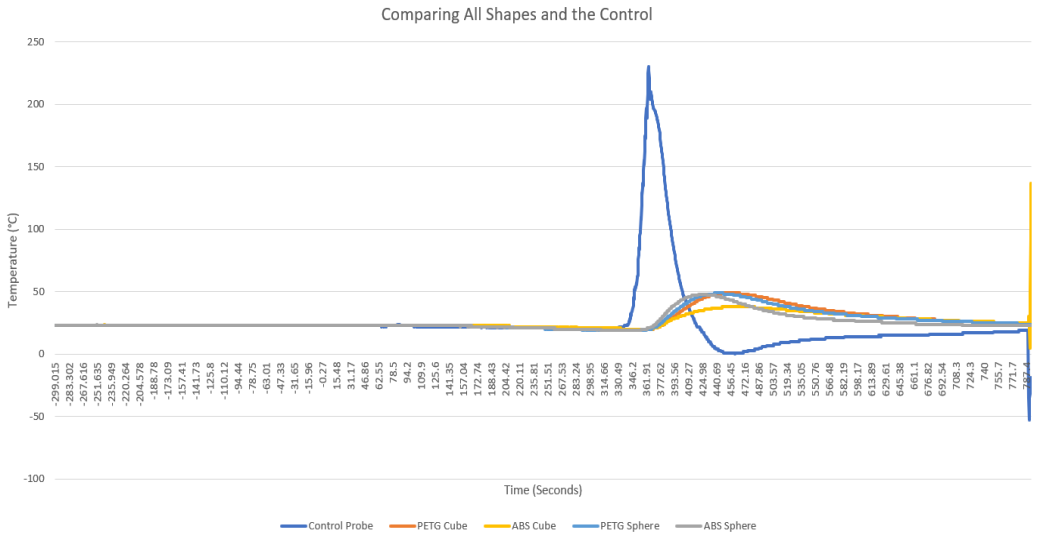

Graph 1: Comparing Internal Temperatures of All Shapes with the Control

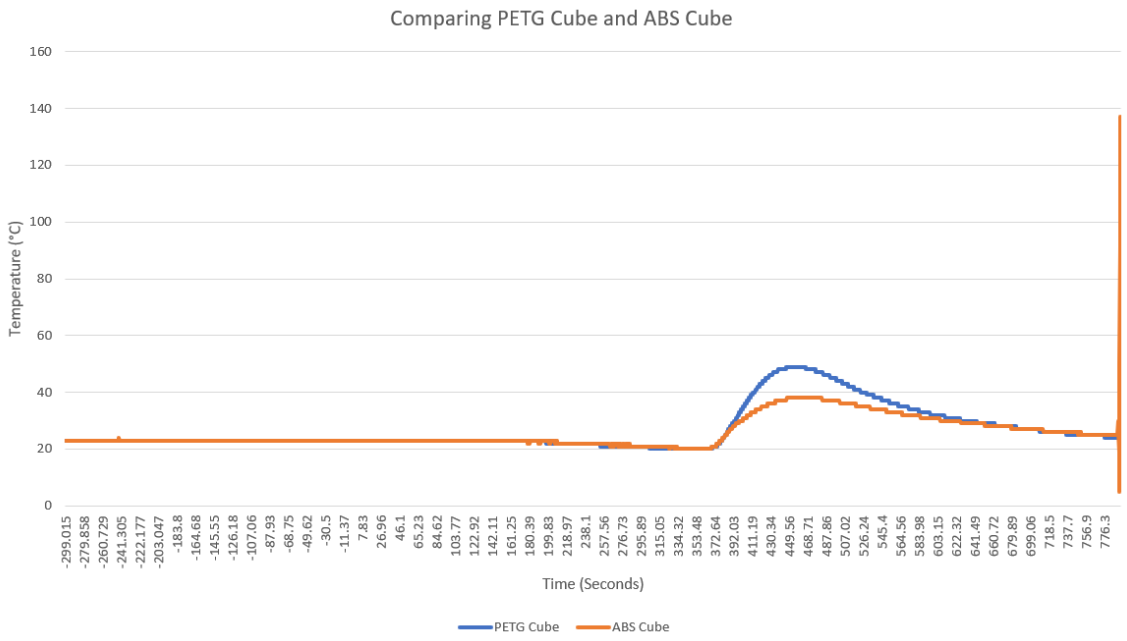

Graph 2: Comparing Internal Temperatures of PETG and ABS Cubical Shapes

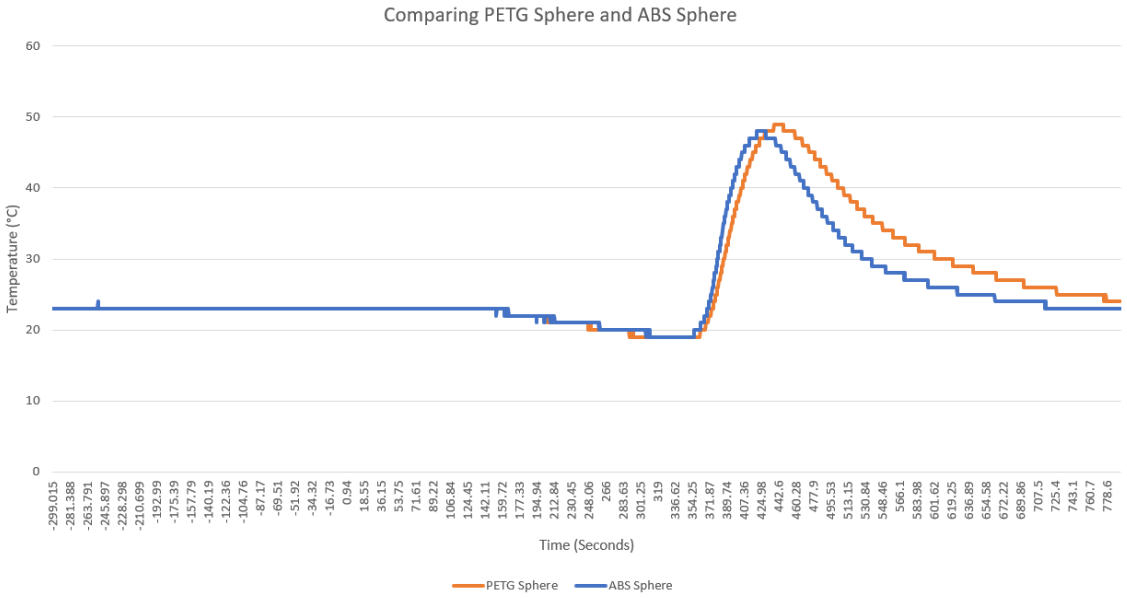

Graph 3: Comparing Internal Temperatures of PETG and ABS Spherical Shapes

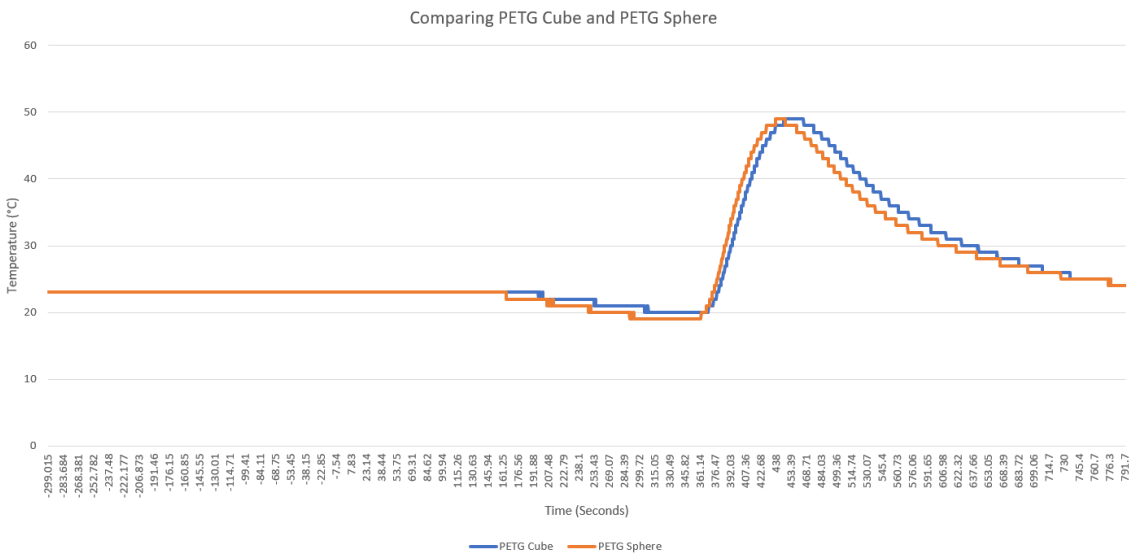

Graph 4: Comparing Internal Temperatures of PETG Cubical and Spherical Shapes

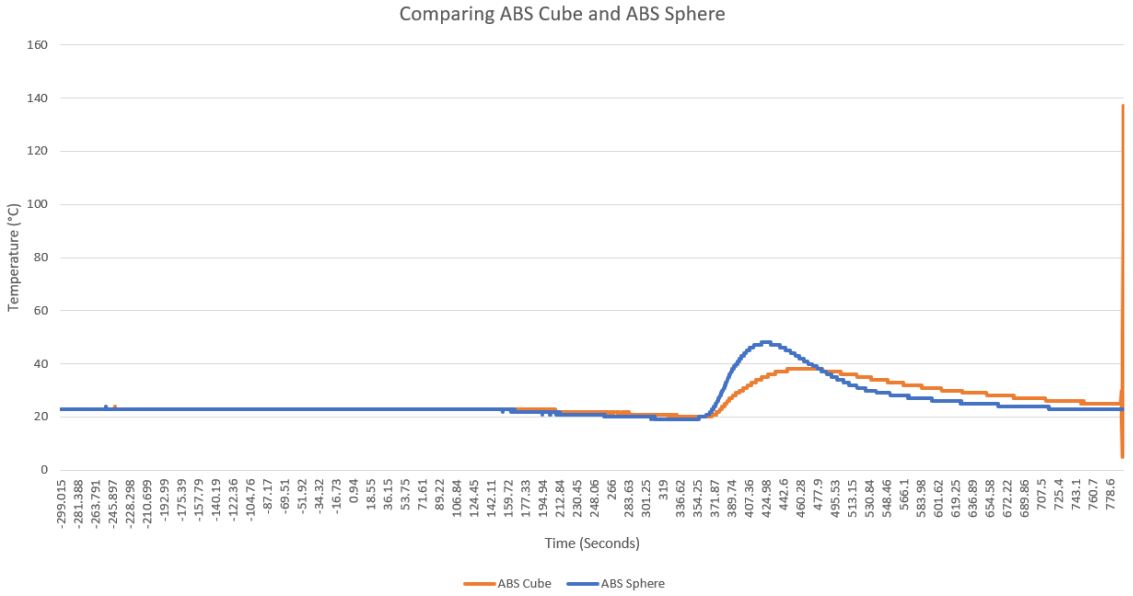

Graph 5: Comparing Internal Temperatures of ABS Cubical and Spherical Shapes

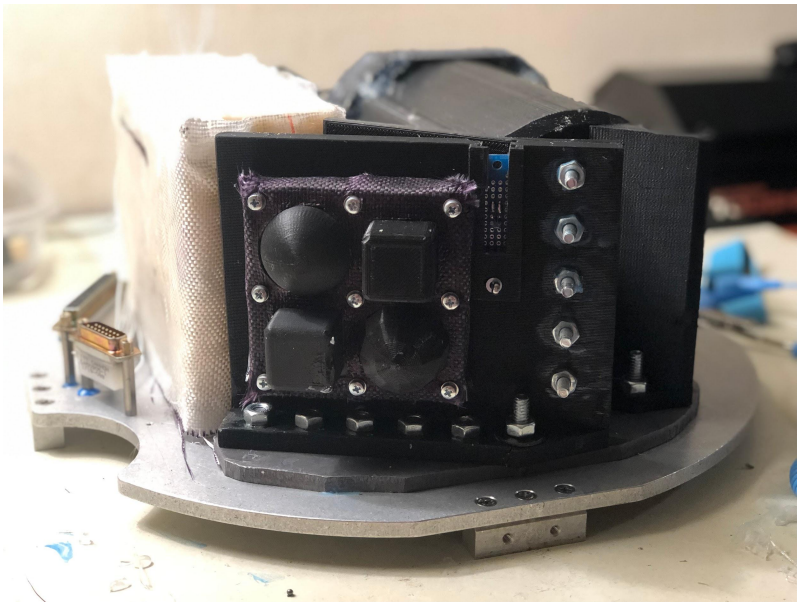

Figure 23:Secondary View Before Flight

7.0 Conclusions

7.1 Primary Experiment Conclusions

After reviewing the camera footage and the data gathered from telemetry, no conclusions could be made from our primary experiment. Pixel values gathered from the telemetry show that there were objects moving, however the data does not correlate with what we would expect. The values stored are essentially an x, y, z coordinates indicating the depth of the BB and it's position. The values that were collected are inconsistent and do not match with the values gathered during our testing. This could be due to the sensitivity of the camera, the camera could have picked up a light source or a different object. These inconsistencies in both the cameras, along with the lack of footage, our primary experiment is inconclusive.

We can however make predictions on what we would have expected to see had the data been accurate. During ground testing, we saw a strong attraction from the BB to the charged polycarbonate plate. When these same test conditions were conducted in a vacuum, the attraction was no longer present, hence the creation of the EAC. When repeating the same test conditions but now with the EAC, the attraction of the free hanging BB and the charge plate were seen once again. The BB and the charged plates behaved like magnets, once close enough the forces between them rapidly grew, this shows that the theoretical math of electrical fields supports our experiment. The EAC was carefully sealed and tested in numerous conditions until we found the perfect procedure to obtain a sealed container. Assuming that the EAC stayed sealed during flight and that the attraction between

the BB and the charged plate remained present, the primary experiment would be proved successful; static electricity is a viable way to change the trajectory of non-ferrous space debris. The experiment should be reconducted with improved data measuring methods to ensure that this statement is accurate.

7.2 Secondary Experiment Conclusions

The secondary experiment collected thermal data upon reentry. The experiment contained two spherical and cubic shapes printed from PETG and ABS 3D filament. Housed inside a hollow section of these shapes was an RTD temperature probe to measure the internal temperature. Aside these printed shapes sat another RTD temperature probe which served as a control. The secondary experiment began upon GSE start up which was approximately T-minus 300 seconds and continued to record temperature data until after splashdown. When analyzing the numerical data of the secondary experiment the control probe gives a clear indication when launch occurred, when apogee was met, when reentry heat was at its peak and when splashdown occurred (Graph 1). A few seconds before shoot deployment the temperature experienced on the payload was 230°C. At this same time the internal temperatures of our test subjects only read 20°C. 56 seconds after the peak of the control, the ABS sphere reached its maximum temperature of 48°C. 74 seconds after the peak temperature of the control, the PETG sphere reached its maximum temperature of 48°C. 86 seconds after the peak of the control the PETG cube and the ABS cube reached their highest internal temperature of 49°C and 38°C respectively. It can be assumed that the shapes didn't report their highest temperature at the same time as the control because the shapes were on fire. The high external temperature was likely burning through the material and did not stop until after shoot deployment and splashdown. Given that there was no notable differences in the shapes appearance, the quantitative data shows that the ABS cubic structure withheld the best from the high temperatures on reentry. Not only did it report the lowest internal temperature but it also took the longest for the heat to penetrate through the structure.

8.0 Potential Follow-on Work

There is a lot that the team has learned from the results of our experiments and there is still a lot to discover. It is important to better understand the effects of reentry and to determine reliable, cost effective materials for future space flight. We received very reliable data from our secondary experiment, the next steps would be to take the experiment to new heights and expand the concept. The sounding rocket only reached an apogee of about 100 miles thus it's reentry energy is not as great as a full descend from outside of Earth's atmosphere. Given the opportunity and funding the next steps to expand the testing of this experiment would be to test and catalog the effects of reentry from a higher descend. The printed structures will likely be exposed to a higher wind velocity and temperature

which will affect their strength, insulative properties, and deformation. The secondary experiment can go as far as testing 3D printed material while in space for a certain duration to measure the effects of radiation, extreme cold, and the rate of decay of the filaments.

As space travel continues, the number of space debris will continue to grow. It is imperative that the necessary steps are taken to deorbit the debris. The primary experiment showed promise during our pre-flight testing and while the flight data did not fully capture or prove the concept, we strongly believe that the use of static electricity is a viable option to change the trajectory of small low earth orbital debris. The team plans to continue testing and exploring this concept. The next steps for this project are to determine how we can get better data in the future. We will then explore static charge in a vacuum state, determine more efficient ways to generate an electric field, and redesign our parts to accommodate our findings.

9.0 Benefits to the Scientific Community

As participants in a global effort to prevent harmful repercussions associated with increasing space debris, our project mission was to design, implement and fly a sounding rocket payload that will collect robust, foundational data to develop passive, cost-effective methodology for de-orbiting small, fragmented space debris using a platform of electrostatic repulsion and incorporating material properties of 3D printed components. Arapahoe Community College, Community College of Aurora, and Red Rocks Community College working in collaboration have developed D.O.T.T.S. (Debris Orbital Tumbler and Thermal Sensors), an experimental payload which contains two experiments: 1. Implementation and use of a static electric field to meaningfully impact the trajectory of simulated space debris fragments. 2. Testing and documentation of key characteristic material properties (internal temperature, shear strength, and deformation) on the effects of thermal reentry on multiple 3D printed structures and varied filaments. Our hope is to contribute meaningful data to the research and development of space remediation and gain a foundational understanding of systems engineering and integration.

The aggregate of space debris orbiting the earth has grown exponentially over the past two decades, an alarming trend with potentially catastrophic impacts on global aerospace activity [1,2]. According to Holger Krag, head of the European Space Agency's (ESA) Space Debris Office, approximately 60 percent of missions follow the International guidelines for removal of spacecraft from low-Earth orbit (LEO) within 25 years of mission completion [1]. The current debris load will require the removal of more than 100 objects from LEO at a minimum rate of five per year to “stop the proliferation of fragments resulting from in-orbit collisions and explosions,” says Satomi Kawamoto, of the Japan Aerospace Exploration Agency (JAXA) [1]. Currently, the U.S. Space

Surveillance Network tracks 1,200 intact, operational satellites, and 18,000 objects larger than 4 inches (~10 centimeters) but estimates that about 750,000 "flying bullets" (~1 centimeter) and roughly 150 million fragments (~1 millimeter) are orbiting earth, which could damage operational satellites [3]. In 1978, Donald J Kessler, a scientist at NASA, predicted the finite area in LEO available to satellites coupled with the growing number of satellites, would lead to an inevitable, self-sustaining cascade of collisions which has far-reaching negative impacts on space exploration [4].

As participants in a global effort to prevent these consequences, our project mission was to design, implement and fly a sounding rocket payload that will collect robust, foundational data to develop passive, cost-effective methodology for de-orbiting small, fragmented space debris using a platform of electrostatic repulsion and additive manufacturing.

10.0 Lessons Learned

Being part of a team that was geographically segregated amongst three community colleges that composed our 15 team member team, there were many things that were learned from this experience. When referring back to our mission statement and while analyzing the data obtained, our team noticed that sometimes even the most precise planning can come with flaws. Our primary experiment experienced vital issues which vandalized our desired results. This caused our team to not meet this part of our mission fully since we were not able to prove nor deny that a static electric charge can change the trajectory of space debris fragments. It could be inferred that components of this particular part of the experiment might have been affected by the force of launch which caused our deployables to not be able to be tracked by our cameras. This taught us what to expect in microgravity being that this was the only thing that was not able to be tested on earth. Our experiment was very successful; we received our temperature data and were able to physically inspect the experiment upon its retrieval.

Aside from these learning components, it could also be said that all the team members grew as individuals. All of the team members were involved in one way or another without putting a main focus to our previous strengths. Some of us wanted to improve our skills in different sectors which allowed us to split accordingly in order to learn new concepts while making positive contributions to the team. Communication was another skill that played a huge part in understanding meetings, payload development, part manufacturing and team dynamics. Good communication helped a lot of team members work through problems that were causing friction between themselves, and helped lead to a more harmonious outcome. Time management is another thing a lot of us learned quickly. Balancing a project that was so demanding and in need of such attention,

with heavy class loads and homework assignments, was something we had to figure out quickly in the beginning. If this payload were to be flown again, something that would not be allowed would be using lower quality manufacturing materials for vital components to the experiment such as the launcher tower or using higher quality printers to ensure consistent design prints. Our team would manufacture a stronger and better developed launcher since this was the only component that was completely destroyed from our payload.

As per our secondary experiment, we had set out to see which of two 3D printer material would withstand the transfer of heat from re-entry the best. As per the data above, the ABS was much better in dissipating the heat and keeping the probe at a cooler level. This shows that in the future, if we were to fly again, ABS would be best to hold up against the harsh conditions of reentry. Along with another, more durable design, if we were to 3D print the launch tower, it would definitely be printed out of ABS material.

11.0 References

[1] Pultarova, Tereza. "Meet the Space Custodians: Debris Cleanup Plans Emerge." Space.com, Future US Inc, 26 Apr. 2017, www.space.com/36602-space-junk-cleanup-concepts.html.

[2] Popova, Rada, and Volker Schaus. "The Legal Framework for Space Debris Remediation as a Tool for Sustainability in Outer Space." Aerospace, vol. 5, no. 2, 2018, p. 55., doi:10.3390/aerospace5020055.

[3] ESA. "Space Surveillance and Tracking - SST Segment." European Space Agency, Http://Www.esa.int, 11 Nov. 2017, www.esa.int/Our_Activities/Operations/Space_Situational_Awareness/Space_Surveillance_and_Tracking_-_SST_Segment.

[4] Kessler, Donald J., and Burton G. Cour-Palais. "Collision Frequency of Artificial Satellites: The Creation of a Debris Belt." Journal of Geophysical Research, vol. 83, no. A6, 1 June 1978, pp. 2637–2646., doi:10.1029/ja083ia06p02637.

[5] Rossi, Alessandro, et al. "ReDSHIFT: A Global Approach to Space Debris Mitigation." Aerospace, vol. 5, no. 2, 2018, p. 64., doi:10.3390/aerospace5020064.

[6] Schaub, Hanspeter, and Zoltán Sternovsky. "Active Space Debris Charging for Contactless Electrostatic Disposal Maneuvers." Advances in Space Research, vol. 53, no. 1, Jan. 2014, pp. 110–118., doi:10.1016/j.asr.2013.10.003.

[7] National Research Council. 2014. 3D Printing in Space. Washington, DC: The National Academies Press. https://doi.org/10.17226/18871.

[8] Werner, Debra. "3D Printing Saving Satellite Builders Time and Money." SpaceNews.com, Space News, 9 Mar. 2017, spacenews.com/3d-printing-saving-satellite-builders-time-and-money/.